Thresholds for leaf damage due to dehydration: declines of hydraulic function, stomatal conductance and cellular integrity precede those for photochemistry

Santiago Trueba[1] (iD), **Ruihua Pan[1,2], Christine Scoffoni[1,3]** (iD), **Grace P. John[1,4]** (iD), **Stephen D. Davis[5] and Lawren Sack[1]** (iD)

[1]Department of Ecology and Evolutionary Biology, University of California Los Angeles, 621 Charles E. Young Drive South, Los Angeles, CA 90095, USA; [2]School of Ecology and Environment, Inner Mongolia University, 235 University West Road, Hohhot, Inner Mongolia 010021, China; [3]Department of Biological Sciences, California State University Los Angeles, 5151 State University Drive, Los Angeles, CA 90032, USA; [4]Department of Integrative Biology, University of Texas at Austin, 2415 Speedway, Austin, TX 78712, USA; [5]Natural Science Division, Pepperdine University, Malibu, CA 90263-4321, USA

Summary

- Given increasing water deficits across numerous ecosystems world-wide, it is urgent to understand the sequence of failure of leaf function during dehydration.
- We assessed dehydration-induced losses of rehydration capacity and maximum quantum yield of the photosystem II (F_v/F_m) in the leaves of 10 diverse angiosperm species, and tested when these occurred relative to turgor loss, declines of stomatal conductance g_s, and hydraulic conductance K_{leaf}, including xylem and outside xylem pathways for the same study plants. We resolved the sequences of relative water content and leaf water potential Ψ_{leaf} thresholds of functional impairment.
- On average, losses of leaf rehydration capacity occurred at dehydration beyond 50% declines of g_s, K_{leaf} and turgor loss point. Losses of F_v/F_m occurred after much stronger dehydration and were not recovered with leaf rehydration. Across species, tissue dehydration thresholds were intercorrelated, suggesting trait co-selection. Thresholds for each type of functional decline were much less variable across species in terms of relative water content than Ψ_{leaf}.
- The stomatal and leaf hydraulic systems show early functional declines before cell integrity is lost. Substantial damage to the photochemical apparatus occurs at extreme dehydration, after complete stomatal closure, and seems to be irreversible.

Introduction

The increasing frequency and severity of declines in precipitation result in critical drought events and hydrological imbalances (Trenberth *et al.*, 2014), inducing tree mortality and shifting species distributions across global ecosystems (Breshears *et al.*, 2005; Allen *et al.*, 2010, 2015). The impacts of drought over large surfaces in crops and natural ecosystems can be evaluated using remotely sensed estimation of canopy water content based on light absorption assessed from hyperspectral measurements (Asner *et al.*, 2016). Yet, such impacts may represent extreme dehydration, beyond the point at which major functions have declined. Indeed, there has been fragmentary knowledge of the sequence of dehydration-induced reduction of stomatal conductance, leaf hydraulic transport, cellular integrity, and chloroplast function. Clarifying thresholds in key physiological functions can thus be important for inferring leaf-level mechanisms, the significance of declines inferred from remotely sensed variables, and for

the improvement of ecosystem-wide models (Adams *et al.*, 2017). A recent meta-analysis has refined hypotheses for how plant organs differ in their water status thresholds for dysfunction under drought stress (Bartlett *et al.*, 2016). However, extensive measurements on a given set of species are necessary to test that sequence, and especially to resolve the placement of irreversible leaf damage. We aimed to integrate key stomatal, photosynthetic, hydraulic, turgor loss, and damage processes into a unified sequence of leaf response to drought for 10 diverse angiosperm species.

Most leaf water exchange occurs through the stomatal pores. Stomatal sensitivity to dehydration can be assessed by measuring the behavior of stomatal conductance g_s (see Table 1 for a list of abbreviations and units) under decreasing water status (Klein, 2014). Declines of g_s with declining values of total relative water content (RWC; combining apoplastic and symplastic water contents) and leaf water potential Ψ_{leaf}, are expected to reduce water loss and to avoid reaching dangerous xylem tensions (Meinzer

et al., 2009). Other traits indicating drought-induced hydraulic dysfunction include the water status at wilting or turgor loss point (TLP; Bartlett et al., 2012a) and the decline of leaf lamina hydraulic conductance K_{leaf}, a major determinant of plant drought responses and ecological preferences (Blackman et al., 2009; Nardini & Luglio, 2014; Scoffoni & Sack, 2017). A key impact of outside-xylem hydraulic conductance K_{ox} in driving whole-leaf hydraulic decline with dehydration has been recently emphasized (Scoffoni et al., 2017). Recent work has suggested that xylem-specific hydraulic decline K_x occurs only after stomatal closure (Hochberg et al., 2017; Scoffoni & Sack, 2017; Skelton et al., 2017a), and a meta-analysis found that most hydraulic traits conferring drought tolerance are correlated (Bartlett et al., 2016). Yet, the Ψ_{leaf} and RWC thresholds inducing TLP, g_s, K_{leaf}, K_{ox}, and K_x declines have not been integrated and directly compared experimentally.

Several studies have shown that stomatal pores reopen after plant rehydration, and reopening is associated with the recovery of K_{leaf} and gas exchange (Miyashita et al., 2005; Blackman et al., 2009; Brodribb & Cochard, 2009; Martorell et al., 2014; Cai et al., 2015; Li et al., 2016; Skelton et al., 2017b). However, in contrast to g_s, there may be limited recovery of photochemistry and mesophyll conductance after rehydration, which constrain full recovery of overall photosynthetic rate (Miyashita et al., 2005; Galmés et al., 2007). The decline of leaf photochemical performance under water deficit can be estimated by the measurement of Chl fluorescence (ChlF) (Baker, 2008). Among the ChlF parameters, the decline of the maximum quantum efficiency of photosystem II (PSII) photochemistry (F_v/F_m) represents the light-harvesting function of the chloroplast (Murchie & Lawson, 2013), and is a parameter that can be used as an index of drought-induced injury in leaves (Guadagno et al., 2017). Previous studies have reported that that PSII photochemistry was little affected by decreasing RWC between 100% and 50% (Genty et al., 1987; Lawlor & Cornic, 2002). Dehydration causes

changes in cell volume and osmotic concentration that can lead to significant structural damage; therefore, we analyzed the percentage loss of F_v/F_m (PLCF) as a proxy of dehydration-induced chloroplast dysfunction within the sequence of dehydration effects.

Under strong dehydration, vegetative tissues may experience irreversible cellular damage. Irreversible mesophyll damage has been assessed by dehydrating tissues and testing their ability to rehydrate (i.e. their loss of rehydration capacity). Irreversible injury in evergreen Mediterranean leaves has been proposed to occur at a percentage loss of rehydration capacity (PLRC) of $\geq 10\%$ (Oppenheimer, 1963; Oppenheimer & Leshem, 1966). The rehydration technique to estimate loss of viability was recently refined and applied to 18 southern California species, showing that water status thresholds for PLRC are related to other drought tolerance indicators and leaf structural traits such as TLP and leaf mass per area (LMA; John et al., 2018). Moreover, thresholds for PLRC varied across biomes, suggesting that leaf rehydration capacity may predict drought tolerance across species (John et al., 2018).

Dehydration-response thresholds can be expressed in terms of declining RWC or Ψ_{leaf}. Which of these water status variables is more directly sensed by leaf cells, and more active in triggering dehydration-induced responses, has been controversial. Whereas Ψ_{leaf} declines reflect xylem tensions that would trigger air seeding and reduction of K_x, there is no clear understanding yet of the direct mechanisms by which low leaf water status drives declines of stomatal closure, K_{ox} and K_{leaf}, along with PLRC or PLCF, and thus it is uncertain whether RWC or Ψ_{leaf} would be most meaningful (Sack et al., 2018). Indeed, some have suggested that RWC might better represent the water status that is sensed by cells experiencing dehydration (Sinclair & Ludlow, 1985), especially as the decline of RWC appears to be critical in the accumulation of the hormone abscisic acid (ABA), consequently driving important physiological responses such as stomatal closure (Brodribb & McAdam, 2011; Sack et al., 2018). Further, species that diverge in thresholds of dehydration responses in terms of Ψ_{leaf} may show convergence in thresholds in terms of RWC (Sack et al., 2018). The incorporation of drivers of physiological responses to dehydration, whether expressed in terms of Ψ or RWC, into predictive models is critical to understand and predict ecosystem responses to drought (Anderegg et al., 2017).

We analyzed the dehydration-induced loss of leaf rehydration capacity, and F_v/F_m along with stomatal conductance and other indices of leaf dehydration tolerance previously measured on the same individuals, for 10 species with diverse sensitivities to water deficit. Using these leaf dehydration responses, we tested key hypotheses: (1) the declines of leaf rehydration capacity and photochemistry vary across species and occur after stomatal closure and decline of leaf hydraulic conductance; (2) F_v/F_m may not recover after rehydration due to permanent dehydration-induced damage; (3) across-species, water status thresholds for loss of stomatal, hydraulic, and photochemical function and cell integrity will be correlated; (4) thresholds in terms of Ψ_{leaf} will be more variable across species than in terms of RWC. Addressing these hypotheses resulted in a comprehensive 'timeline' of leaf

Table 1 Symbols and definitions of water status indices and thresholds measured.

Symbol	Definition	Units
RWC	Relative water content	%
Ψ_{leaf}	Leaf water potential	MPa
F_v/F_m	Maximum quantum efficiency of photosystem II photochemistry	Unitless
K_{leaf}	Leaf hydraulic conductance	$mol\ m^{-2}\ s^{-1}\ MPa^{-1}$
K_{ox}	Outside-xylem leaf hydraulic conductance	$mol\ m^{-2}\ s^{-1}\ MPa^{-1}$
K_x	Xylem vein leaf hydraulic conductance	$mol\ m^{-2}\ s^{-1}\ MPa^{-1}$
g_s	Stomatal conductance	$mmol\ m^{-2}\ s^{-1}$
PLRC	Percentage loss of rehydration capacity	%
PLCF	Percentage loss of Chl fluorescence (F_v/F_m)	%
TLP	Turgor loss point	MPa
LA	Leaf area	cm^2
LMA	Leaf mass per area	$g\ m^{-2}$

functional impairment with decreasing leaf water status during drought stress.

Materials and Methods

Plant material

We studied 10 angiosperm species varying in leaf hydraulic vulnerability and drought tolerance (Table 2; Guyot *et al.*, 2012; Scoffoni *et al.*, 2017, 2011). Measurements were made from December 2016 to April 2017 on three mature individuals per species. Individuals are located in the campus of University of California Los Angeles and Will Rogers State Park, Los Angeles, California. Sun-exposed shoots 20–65 cm in length were collected early in the morning, to avoid native embolisms, and immediately transported to the laboratory in dark plastic bags containing moist paper towels, recut underwater by three nodes, placed with cut ends under water, and rehydrated overnight covered in plastic for > 12 h. Thirteen fully expanded leaves per individual were excised from the shoots, avoiding leaves with pathogen or herbivore damage. Previous studies have shown similar hydraulic declines under dehydration alternatively using bench-dried shoots or droughted plants (Blackman *et al.*, 2009; Pasquet-Kok *et al.*, 2010). We therefore used a bench-drying approach to assess dehydration impacts on hydraulic, rehydration, and photochemistry capacities. To isolate the effect of water scarcity on leaf function, dehydration for all measurements was carried out at room temperature and low irradiance levels, with a range in photosynthetic photon flux density of 4–19 µmol m^{-2} s^{-1}, and temperature and relative humidity ranges of 20–25°C and 35–45%, respectively.

Determination of relative water content and water status thresholds for loss of rehydration capacity

Fully turgid leaves were weighed immediately after excision using an analytical balance (± 0.01 mg; AB265-S; Mettler Toledo, Greifensee, Switzerland). ChlF was measured promptly

after weighing, as described in the following section. The projected leaf area (LA, cm^2) was measured with a leaf area meter (LI-3100; Li-Cor Biosciences, Lincoln, NE, USA) or scanned with a flatbed scanner (Canon Scan Lide 90; Canon, New York, NY, USA) and measured using IMAGEJ v.1.51h (NIH Image; Bethesda, MD, USA). Leaves were then placed over a bench fan to dehydrate under ambient light. Three randomly selected leaves were removed from the drying bench at different time points to represent a gradual dehydration gradient and measured for LA and ChlF. Species varied in the times necessary for dehydration depending on their water loss rates; for instance, the thin leaves of *Lantana camara* and *Salvia canariensis* required only 24 h to reach very low water contents, whereas *Magnolia grandiflora* required up to 10 d. Dehydrated leaves were placed in water-filled 15 ml polypropylene tubes (Fisher brand; Fisher Scientific Co., Waltham, MA, USA), covered, and rehydrated overnight. Only the petioles of leaves were immersed under water, avoiding contact of the leaf blades with water, for 10–12 h rehydration, longer than the minimum of 8 h of rehydration required (John *et al.*, 2018). LA, mass, and ChlF were then measured on the rehydrated leaves. Finally, leaves were oven dried at 70°C for 72 h and leaf dry mass was determined. LMA (g m^{-2}) was determined by dividing the dry leaf mass by the area of the turgid leaf.

We calculated the saturated water content (SWC, g g^{-1}) of saturated (i.e. fully turgid before dehydration) and rehydrated leaves as:

$$SWC_s = \frac{M_s - M_d}{M_d} \qquad \text{Eqn 1}$$

$$SWC_r = \frac{M_r - M_d}{M_d} \qquad \text{Eqn 2}$$

where M_d, M_s, and M_r are the mass values (in grams) of dry, saturated (i.e. fully turgid), and rehydrated leaves, respectively. The SWC of rehydrated leaves and saturated leaves were used to calculate the percentage loss of rehydration capacity (PLRC, %) as:

Table 2 List of measured angiosperm species, values of leaf structural variables, and thresholds of dehydration tolerance.

Species	Family	Native biome and origin	Leaf area (cm^2)	Leaf mass per area (g m^{-2})	RWC (%) at:			
					PLRC$_{10}$	PLRC$_{50}$	PLCF$_{10}$	PLCF$_{50}$
Cercocarpus betuloides	Rosaceae	Mediterranean, North America	8 ± 0.31	314 ± 12	58.97	36.86	65.26	4.94
Comarostaphylis diversifolia	Ericaceae	Mediterranean, North America	9 ± 0.53	306 ± 8	57.27	35.61	40.38	26.46
Hedera canariensis	Araliaceae	Temperate forest, Africa	44 ± 3.60	71 ± 3	78.42	45.47	25.27	8.81
Heteromeles arbutifolia	Rosaceae	Mediterranean, North America	18 ± 1.22	138 ± 3	67.92	36.78	28.52	15.02
Lantana camara	Verbenaceae	Tropical dry forest, pantropical	15 ± 0.68	65 ± 2	63.81	34.18	30.18	8.98
Magnolia grandiflora	Magnoliaceae	Temperate forest, North America	45 ± 2.18	256 ± 4	83.05	43.29	99.55	28.58
Malosma laurina	Anacardiaceae	Mediterranean, North America	14 ± 0.83	189 ± 3	83.75	43.51	45.75	17.63
Quercus agrifolia	Fagaceae	Mediterranean, North America	9 ± 0.55	205 ± 7	79.60	43.56	43.27	14.69
Rhaphiolepis indica	Rosaceae	Temperate forest, Asia	10 ± 0.41	217 ± 3	62.82	40.27	32.77	14.69
Salvia canariensis	Lamiaceae	Temperate forest, Africa	37 ± 3.69	79 ± 2	66.52	41.75	24.97	8.09

Mean ± SE of leaf structural variables (leaf area, leaf mass per area) are provided. PLCF, percentage loss of Chl fluorescence; PLRC, percentage loss of rehydration capacity; RWC, relative water content.

$$PLRC = 100 \times \left(1 - \frac{SWC_r}{SWC_s}\right) \qquad \text{Eqn 3}$$

The total relative water content (RWC, %) of dehydrated leaves was calculated as:

$$RWC = 100 \times \left(\frac{M_{de} - M_d}{M_s - M_d}\right) \qquad \text{Eqn 4}$$

where M_{de}, M_d, and M_s are the mass values (in grams) of dehydrated, dry, and water saturated leaves, respectively. Rehydration curves for each species were determined by fitting functions to the increase of PLRC with decreasing RWC, as described in the Data analyses section. The RWC at which the 10%, 20%, and 50% of rehydration capacity were lost (RWC at $PLRC_{10}$, $PLRC_{20}$, and $PLRC_{50}$, respectively) were extracted from the rehydration curves.

Maximum quantum yield of PSII and water status thresholds for loss of ChlF

ChlF was measured using a portable pulse-modulated fluorometer (OS1p; Opti-Sciences, Hudson, NH, USA) with a modulated light source of $0.2\,\mu mol\,m^{-2}\,s^{-1}$ at 660 nm and a saturation pulse from a white light-emitting diode with an intensity of $7700\,\mu mol\,m^{-2}\,s^{-1}$ for a duration of 1.5 s. Measurements were performed on the adaxial surface at the middle zone of the leaf blade, avoiding main veins. Leaves were dark adapted for 30 min before measurements using leaf clips to avoid the effects of non-photochemical acute photoinhibition during measurements. The maximum quantum yield of the PSII was estimated as the ratio of variable to maximum fluorescence:

$$\frac{F_v}{F_m} = \frac{F_m - F_o}{F_m} \qquad \text{Eqn 5}$$

where F_m and F_o are respectively the maximal and minimum fluorescence. F_v/F_m indicates the maximum efficiency at which light absorbed by the PSII for reduction of the primary electron acceptor quinone molecule of PSII (Genty et al., 1989). In this study we assessed the percentage loss of ChlF (PLCF, %) as an index of loss of fluorescence capacity after dehydration, using the ratio of F_v/F_m of individual leaves at dehydration, and at saturated status:

$$PLCF = 100 \times \left(1 - \frac{F_v/F_{m\ dehydrated}}{F_v/F_{m\ saturated}}\right) \qquad \text{Eqn 6}$$

We then analyzed the variation of PLCF as a function of RWC to estimate the RWC corresponding to 10%, 20%, and 50% loss in F_v/F_m. We tested F_v/F_m before and after leaf rehydration to determine the recoverability of F_v/F_m. To analyze the recovery of F_v/F_m, we considered four stages of water stress based on the minimum RWC reached during dehydration: operational (stage 1; 100–90% RWC), corresponding to leaves with RWC values above TLP; mild (stage 2; 90–70% RWC);

moderate (stage 3; 70–40% RWC); and severe (stage 4; 40–0% RWC).

Given declines in F_v/F_m during dehydration, we tested the possibility that these arose due to Chl degradation in excited leaves. We measured Chl content during dehydration for a subset of four species with different drought tolerances, *Cercocarpus betuloides*, *Comarostaphylis diversifolia*, *L. camara*, and *Malosma laurina*. Chl concentration of dehydrated leaves was measured using a portable Chl meter (SPAD-502; Minolta Camera Co., Osaka, Japan); (Uddling et al., 2007). Values for Chl concentration were also corrected for the effects of leaf area shrinkage during dehydration by multiplying the values by the ratio of dehydrated leaf area/saturated leaf area.

The test of the decline of F_v/F_m during rehydration was conducted for all 10 species under the ambient light of the laboratory ($7 \pm 2\,\mu mol\,m^{-2}\,s^{-1}$) specifically to isolate the effect of dehydration on leaf photochemistry without excess light and temperature stresses. However, we further tested the effect of dehydration on F_v/F_m under high irradiance for the subset of four species contrasting in drought tolerances, *C. betuloides*, *C. diversifolia*, *L. camara*, and *M. laurina*. Twenty-five leaves per species were dehydrated under a light source with an irradiance of $343 \pm 42\,\mu mol\,m^{-2}\,s^{-1}$, and we measured F_v/F_m using the previously described protocol. We estimated PLCF thresholds of leaves dehydrated under high irradiance and compared these thresholds with those measured under low irradiance.

Stomatal conductance and water status thresholds for stomatal closure

The water status values inducing 20%, 50%, and 80% declines in stomatal conductance g_s were determined for the same individual plants using shoot drying experiments. We measured g_s on the abaxial surface of leaves using a porometer (AP-4; Delta-T Devices Ltd, Cambridge, UK) during progressive dehydration. After porometer measurements, leaves were placed in bags and allowed to equilibrate for a minimum of 30 min before measurement of Ψ_{leaf} using a pressure chamber (Plant Moisture Stress pressure chamber model 1000; PMS Instrument Co., Albany, OR, USA).

Additional hydraulic data used to determine the sequence of functional loss during dehydration

We synthesized the data from previous studies on the same individual plants of the same species for TLP measured using the osmometric method (Bartlett et al., 2012b) and thresholds for leaf hydraulic vulnerability (Scoffoni et al., 2011; Guyot et al., 2012). Additionally, we gathered previously published data of the thresholds for the declines of xylem and outside-xylem hydraulic conductance (K_x and K_{ox}, respectively) for eight of the species studied (Scoffoni et al., 2017). Although interindividual plasticity was eliminated by sampling the exact same individuals, interannual plasticity would introduce a level of uncertainty in the comparison of thresholds. However, such plasticity is not expected to reduce the robustness in our comparison of

thresholds. Interannual comparisons of TLP measurements of the individuals studied showed high similarity in TLP values from different years ($r^2 = 0.88$, for 2012 vs 2016 measurements; $n = 13$; L. Sack, unpublished data). Moreover, previous studies showed similar K_{leaf} vulnerability for at least five species measured in different years (Brodribb & Holbrook, 2003, 2006; Scoffoni *et al.*, 2011; Guyot *et al.*, 2012; L. Sack, unpublished data).

Pressure–volume curves and conversion of water status indices

We estimated dehydration-induced thresholds of leaf damage in terms of both Ψ_{leaf} and RWC. The conversion of Ψ_{leaf} to RWC was employed to determine the RWC thresholds of stomatal conductance and the previously published dehydration tolerance traits (TLP, K_{leaf}, K_{ox}, and K_x). Similarly, we converted the RWC thresholds of PLRC and PLCF measured in this study into Ψ_{leaf} thresholds. For these conversions, we used equations based on pressure–volume curve parameters determined for leaves of the same individual plants using the bench-dry method (Sack & Pasquet-Kok, 2011; Sack *et al.*, 2018). Five leaves per species were measured to determine the relation of Ψ_{leaf} and mass during dehydration. From these curves we determined osmotic potential at turgor loss point π_{tlp} and at full turgor π_o, RWC at turgor loss point RWC_{tlp}, and modulus of elasticity ε. Pressure–volume curve parameters for each species studied are available in the Supporting Information Table S1. Notably, extremely low RWC thresholds (i.e. $< 40\%$) could not be converted into Ψ_{leaf} thresholds using these equations, as this required extrapolation beyond the pressure–volume curve data, which led to unreliable estimates, especially given uncertainty in the estimation of apoplastic fraction (Arndt *et al.*, 2015). Therefore, $\Psi_{PLCF_{10}}$ was only computed for five species, and $\Psi_{PLCF_{50}}$ only for *L. camara*. $\Psi_{PLCF_{50}}$ could be calculated for only three species, and thus these thresholds were not included in further analyses.

Data analyses

The loss of rehydration capacity and ChlF as a function of leaf relative water content was determined by fitting the relationship of the dependent variables PLRC and PLCF against RWC using three differently shaped functions: linear, $y = a + bx$; exponential, $y = a \exp(-bx)$; and sigmoidal, $y = a/\{1 + \exp[-(x - X_o)/b]\}$. Functions were fitted, parameterized and compared using maximum likelihood, and for each species' response the function was selected according to the lowest Akaike information criterion corrected for small n (Burnham & Anderson, 2003). The selected functions were used to estimate 10%, 20%, and 50% losses in rehydration capacity and ChlF for each species. The same procedure was used to estimate Ψ_{leaf} thresholds inducing stomatal closure.

We built a linear-mixed effect model to compare F_v/F_m values in dehydrated and rehydrated leaves with those of water-saturated leaves using the R packages LME4 (Bates *et al.*, 2014) and LMERTEST (Kuznetsova *et al.*, 2017). Hydration treatments were included as fixed effects, whereas species and individuals were included as random effects to account for repeated measures within and across species. Comparisons across hydration stages were assessed using *t*-tests based on Satterhwaite's degrees of freedom method (Kuznetsova *et al.*, 2017). Additionally, differences in F_v/F_m among saturated leaves, leaves dehydrated to different stages of water stress, and rehydrated leaves were assessed using a one-way ANOVA with post-hoc Tukey's honest significant difference using 95% confidence intervals. The same analysis was applied to assess differences in Chl concentration in leaves at different stages of water stress. Differences of F_v/F_m declines of leaves under high vs low irradiance were assessed using a paired *t*-test across the four species tested.

We used both indices of water status, RWC and Ψ_{leaf}, to assemble sequences of thresholds of functional decline and to compare the variability of thresholds among both water status indices. To establish the sequence of drought response thresholds, we used *t*-tests to compare species means for RWC and Ψ_{leaf} thresholds of drought responses. Ψ_{leaf} values were multiplied by -1 to generate positive values for analyses. We assessed the variability of RWC and Ψ_{leaf} thresholds overall by comparing their coefficients of variation (CVs). CV equality was tested using the modified signed-likelihood ratio test (Krishnamoorthy & Lee, 2014), which was implemented using the R package CVEQUALITY (Marwick & Krishnamoorthy, 2016).

We estimated trait–trait relationships across species using correlation analyses on mean species trait values. Correlations were evaluated for both untransformed data and log-transformed data to test approximately linear or curvilinear (i.e. power-law) relationships. When relationships were found between two 'dependent' variables, we fitted standardized major axes to plot these relationships using the R package SMATR (Warton *et al.*, 2012). Our dataset is available in Table S2. All data analyses were carried out using R v.3.4.1 (R Core Team, 2017).

Results

Loss of rehydration capacity with leaf dehydration

Declining RWC strongly reduced leaf rehydration capacity in the 10 study species (Fig. 1). The sigmoid function was selected by maximum likelihood for the relation of PLRC and RWC for most species analyzed, whereas this relation was best explained by a linear function only for *M. grandiflora* (adjusted r^2 of the selected models ranged from 0.93 to 0.98; Fig. 1; Table S3). Most species had relatively slight losses ($< 10\%$) of rehydration capacity until reaching *c.* 70% RWC (Fig. 1), with subsequently strong decreases until reaching a plateau at RWC of *c.* 25% (Fig. 1), after which the loss in rehydration capacity became weaker as RWC approached zero. Across species, the mean RWC values inducing a 10%, 20%, and 50% loss in rehydration capacity were $70 \pm 3\%$, $60 \pm 3\%$, and $40 \pm 1\%$, respectively (mean $\pm$ SE; Table 2). The minimum and maximum $RWC_{PLRC_{50}}$ were 34% and 45%, for *L. camara* and *Hedera canariensis*, respectively (Fig. 1d,e). Indices of leaf rehydration capacity were interrelated: RWC_{PLRC50} was strongly correlated with $RWC_{PLRC_{10}}$ and $RWC_{PLRC_{20}}$ ($r = 0.82–0.85$; $P = 0.002–0.003$). Across species,
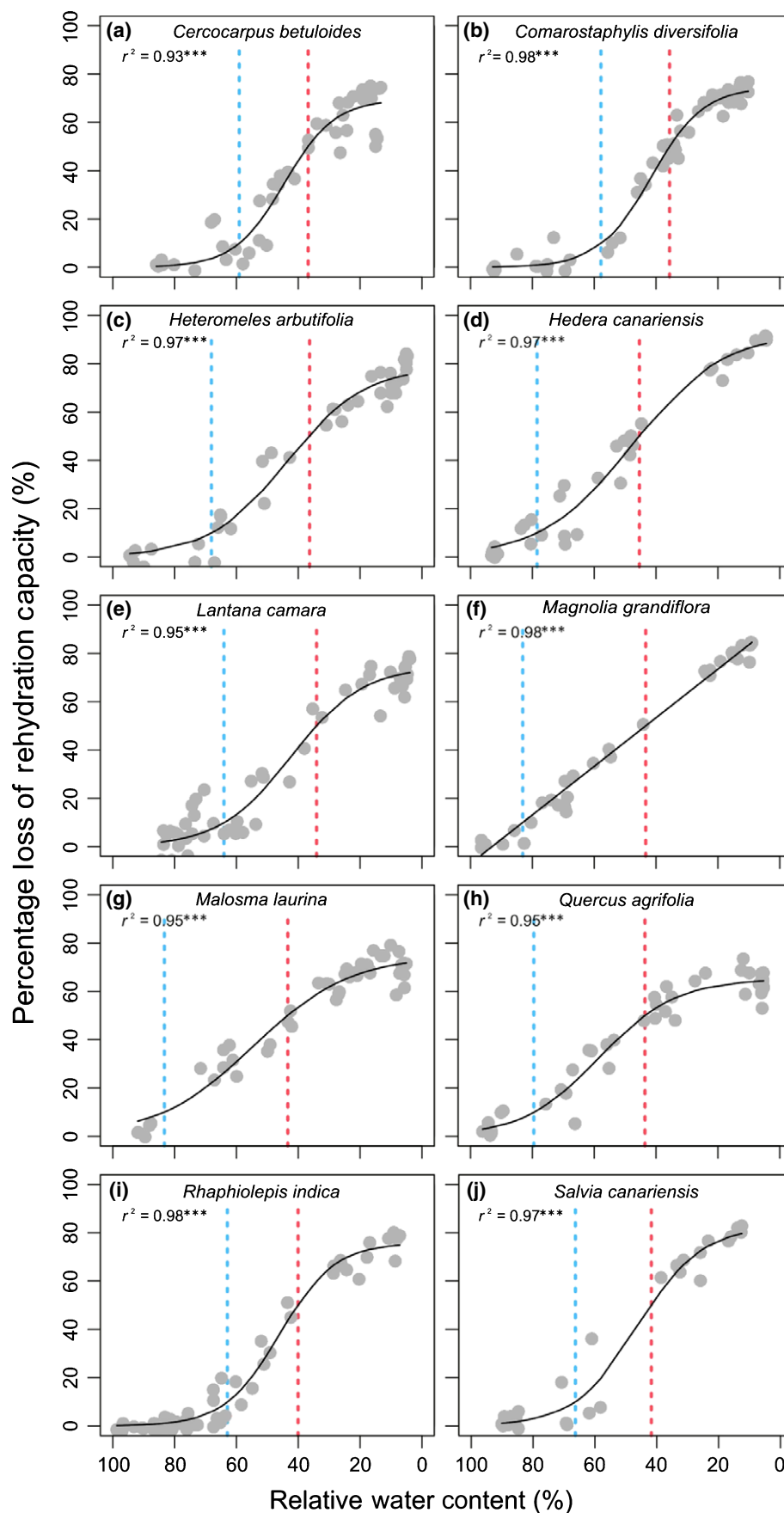
Fig. 1 Response of percentage loss of rehydration capacity (PLRC) over decreasing relative water content (RWC) for the 10 species studied. Gray points are measured leaves, and solid regression lines are best-fit models. The dashed lines in each plot indicate the RWC associated with 10% (blue) and 50% (red) losses of rehydration capacity. ***, $P \leq 0.001$. (a–j) refer to different species in the panel.

mean $\Psi_{PLRC_{10}}$ was -2.71 ± 0.33, and mean $\Psi_{PLRC_{20}}$ was -4.64 ± 0.89, and Ψ_{leaf} thresholds of leaf rehydration were correlated ($r = 0.77$; $P = 0.04$). The RWC and Ψ_{leaf} thresholds of rehydration capacity were statistically independent of LA ($RWC_{PLRC_{50}}$: $r = 0.56$; $P = 0.09$; and $\Psi_{PLRC_{10}}$: $r = 0.15$; $P = 0.74$) and LMA ($RWC_{PLRC_{50}}$: $r = -0.17$; $P = 0.64$; and $\Psi_{PLRC_{10}}$: $r = -0.53$; $P = 0.22$).

Response of PSII yield to dehydration and rehydration

F_v/F_m declined strongly with dehydration to very low RWC (Fig. 2). In most species, percentage losses of F_v/F_m increased exponentially with decreasing RWC (Fig. 2), whereas a sigmoid model was selected for *C. diversifolia* (Fig. 2b), *Heteromeles arbutifolia* (Fig. 2c), and *Quercus agrifolia* (Fig. 2h) (adjusted r^2 ranged from 0.47 to 0.97; Table S4). During the first phases of leaf dehydration, F_v/F_m remained unresponsive to declining RWC (Fig. 2), and in most species the decline in F_v/F_m became substantial only after reaching RWC of *c.* 40%, with dramatic reductions near RWC of 20%. The mean RWC values associated with 10%, 20%, and 50% losses in F_v/F_m were $44 \pm 7\%$, 32 ± 5-%, and $16 \pm 3\%$, respectively (Table 2). *Cercocarpus betuloides* and *M. grandiflora* were the species with the most and least desiccation-resistant photosynthetic light reaction apparatus, with $RWC_{PLCF_{50}} = 5\%$ and $RWC_{PLCF_{50}} = 29\%$, respectively (Fig. 2a,f).

Rehydrated leaves had significantly lower F_v/F_m and did not recover to their initial values (Table S5). F_v/F_m varied significantly across levels of water stress (Fig. 3; ANOVA, $P < 0.05$). However, F_v/F_m did not recover significantly at any level of water stress (Fig. 3). RWC thresholds for PLCF correlated positively with LMA across species, such that species with higher LMA also had a more sensitive photosynthetic light reaction apparatus ($r = 0.64$; $P = 0.048$ for $RWC_{PLCF_{10}}$; $r = 0.67$; $P = 0.033$ for $RWC_{PLCF_{20}}$). RWC thresholds for PLCF were statistically independent of LA. The $\Psi_{PLCF_{10}}$ could be extrapolated only for five species and was -15.2 ± 5.14 MPa on average.

For four species tested for potential Chl concentration decline in dehydrating leaves, we found instead an increase in Chl concentration with dehydration (Fig. S1a). However, after correction for the area shrinkage of leaves during dehydration, we found that Chl concentrations remained constant during dehydration (Fig. S1b).

We tested the influence of high irradiance ($343 \pm 42\ \mu mol\ m^{-2}\ s^{-1}$) vs ambient laboratory irradiance ($7 \pm 2\ \mu mol\ m^{-2}\ s^{-1}$) on the decline of F_v/F_m with dehydration in four species (Fig. 4; Table S4). Although there was an empirical trend for earlier F_v/F_m decline during dehydration under high irradiance (Fig. 4), we found no statistical differences in the RWC thresholds of F_v/F_m decline with irradiance.

Sequence of leaf functional failure during dehydration, and comparisons of threshold variability in terms of RWC and Ψ_{leaf}

We built a sequence of dehydration-induced leaf functional decline as defined by RWC thresholds (Fig. 5). The 20% declines

in leaf hydraulic conductance $K_{leaf\ 20}$ and in stomatal conductance $g_{s\ 20}$ occurred at similar RWC thresholds (Fig. 5; Table S6). The 50% decline of outside-xylem leaf conductance $K_{ox\ 50}$ was followed sequentially by those of $g_{s\ 50}$ and $K_{leaf\ 50}$, which overlapped across the measured species (Fig. 5; Table S6). TLP occurred after the 50% decline of most of the hydraulic traits included in the analysis (Fig. 5; Table S6). However, TLP occurred before substantial limitations in stomatal and leaf hydraulic conductance (Fig. 5). The average thresholds for 80% declines in stomatal conductance overlapped with TLP and with $K_{leaf\ 80}$ (Fig. 5; Table S6), and was followed sequentially by those of $K_{ox\ 88}$, $K_{x\ 50}$, $PLRC_{10}$, $K_{x\ 88}$, $PLCF_{10}$, $PLRC_{50}$, and $PLCF_{50}$.

Declines in rehydration capacity occurred late in the sequence of functional decline (Fig. 5). Most of the declines in hydraulic conductance and stomatal activity occurred before $PLRC_{10}$, with only $K_{x\ 88}$ following in the dehydration-induced injury sequence (Fig. 5), and both traits shared similar RWC thresholds on average across species (Table S6). Finally, declines in F_v/F_m took place at the end of the leaf injury sequence, under high or low irradiance, with $PLCF_{10}$ and $PLCF_{50}$ occurring at very low RWC (Figs 4, 5), and after a substantial decline of the other dehydration tolerance traits considered. Overall, the sequence of dehydration-induced leaf functional impairment was similar across species (Fig. S2) with some differences observed, especially at the first stages of dehydration. In general, Ψ_{leaf} thresholds of leaf functional decline occurred in a sequence similar to those estimated using RWC (Fig. 6; Table S7). All the Ψ_{leaf} thresholds of dehydration responses analyzed had significantly greater variability across species than RWC thresholds did (Table 3). On average, the CV for thresholds based on Ψ_{leaf} were four-fold higher than those based on RWC.

Correlations among thresholds of water status at leaf functional decline

Across species, most RWC thresholds for functional decline tended to be intercorrelated (r values ranged from 0.64 to 0.99; untransformed data; Table S8). In particular, the RWC inducing 50% declines of rehydration capacity ($RWC_{PLRC_{50}}$) was correlated with other thresholds for hydraulic decline and dehydration tolerance traits. Thus, $RWC_{PLRC_{50}}$ was correlated with the RWC thresholds for declines of leaf hydraulic conductance by 10, 20, 50, and 80% ($K_{leaf\ 10}$, $K_{leaf\ 20}$, $K_{leaf\ 50}$, $K_{leaf\ 80}$, respectively; Fig. 7a; Table S8), and the RWC thresholds for decline of outside xylem hydraulic conductance K_{ox} by 50% and 88% (Fig. 7b; Table 4). None of the thresholds for K_x decline were related to those for rehydration capacity (Table 4). $RWC_{PLRC_{50}}$ was also correlated with RWC_{TLP} (Fig. 7c), and RWC_{TLP} was also correlated with other dehydration tolerance traits, including $RWC_{K_{leaf\ 10}}$ and $RWC_{g_{s\ 20,50}}$ (Table S8). RWC thresholds for loss of F_v/F_m (RWC_{PLCF}) were uncorrelated with those for leaf hydraulic decline and TLP (Table 4). However, $RWC_{PLCF_{50}}$ was correlated with RWC thresholds of stomatal conductance decline (Table 4). Thresholds for functional decline in terms of Ψ_{leaf} were also intercorrelated; that is, $\Psi_{PLRC_{10}}$ with Ψ_{TLP} ($r = 0.93$;
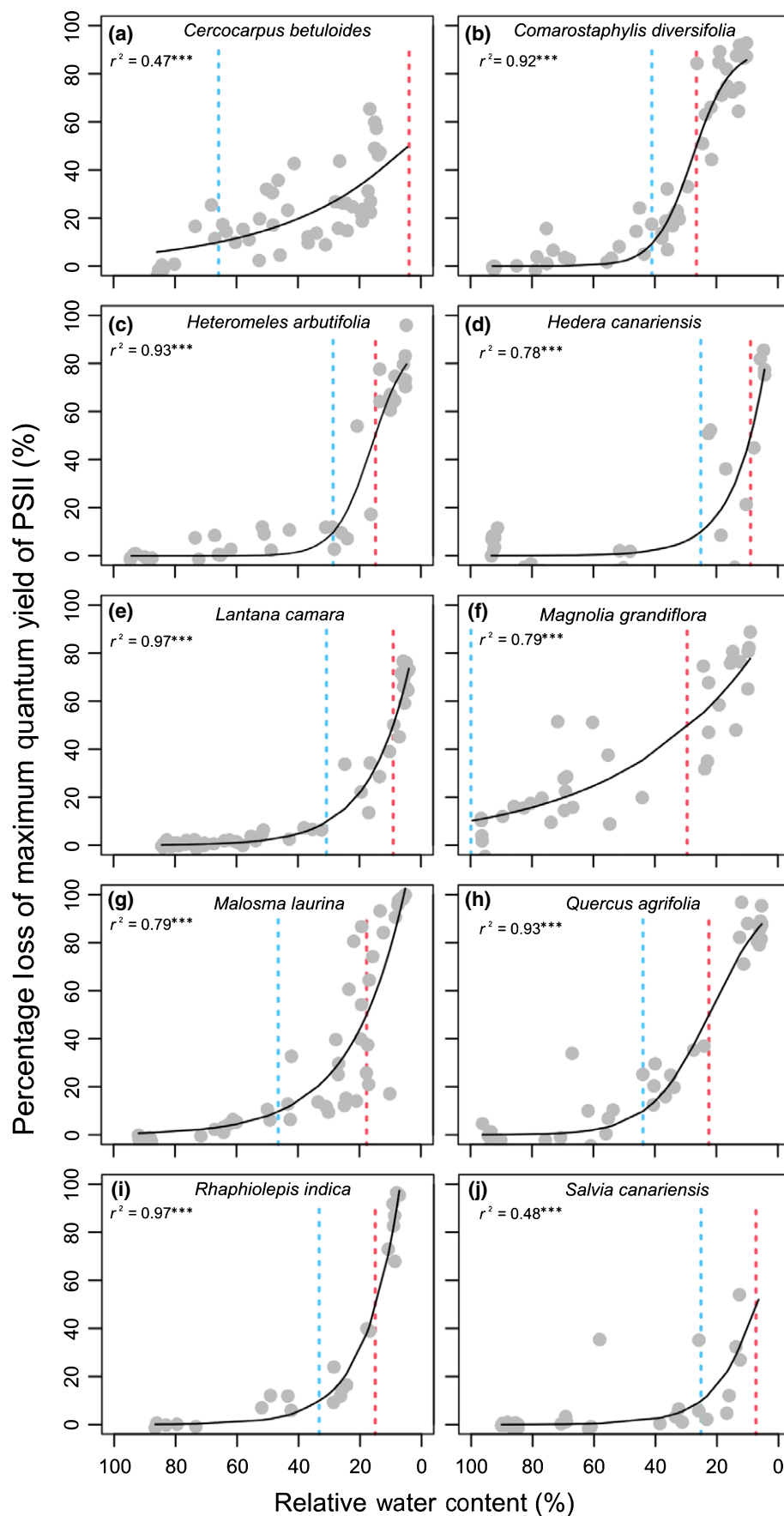
Fig. 2 Response of percentage loss of maximum quantum yield of photosystem II (F_v/F_m; noted in the text as PLCF) over decreasing relative water content (RWC) for the 10 species studied. Gray points are measured leaves and solid regression lines are best-fit models. The dashed lines in each plot indicate the RWC associated with 10% (blue) and 50% (red) losses of F_v/F_m. ***, $P \leq 0.001$. (a–j) refer to different species in the panel.
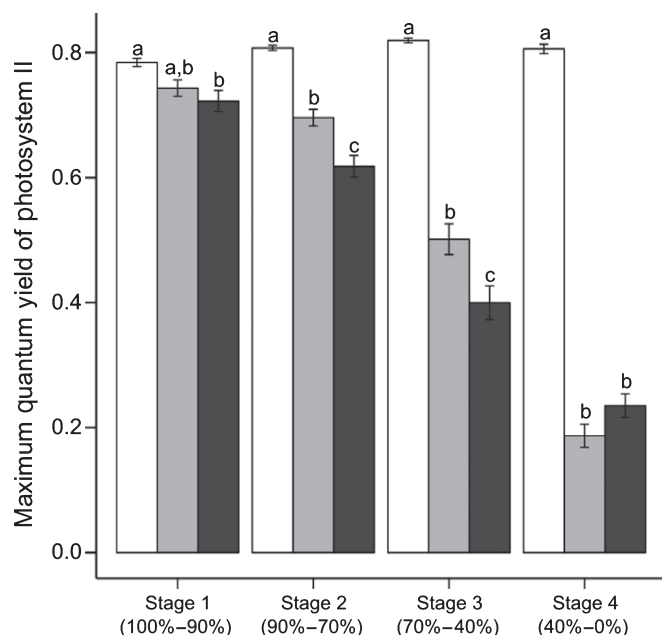
Fig. 3 Maximum quantum yield of the photosystem II (F_v/F_m) of 10 angiosperm species at different stages of water stress. Ranges of leaf relative water content (RWC) for each water status are included in parentheses. Bars represent mean ($\pm$ SE) values at full turgor (white bars), dehydrated (light gray), and after rehydration (dark gray). Letters indicate significant differences at a 0.95 confidence level.
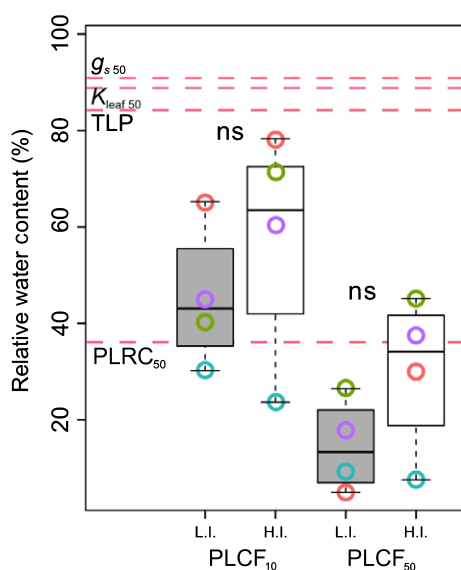

Fig. 4 Differences between indices of percentage loss of Chl fluorescence (F_v/F_m) of dehydrating leaves measured under low (7 ± 2 µmol m^{-2} s^{-1}; gray boxes) vs high (343 ± 42 µmol m^{-2} s^{-1}; white boxes) irradiance. Colored points represent index values for each species. Measurements were carried out on a subset of four species: *Cercocarpus betuloides* (red), *Comarostaphylis diversifolia* (green), *Lantana camara* (blue), and *Malosma laurina* (purple). Boxes indicate median, quartiles, minimum and maximum values for each index of Chl fluorescence decline. Dashed horizontal lines represent the occurrence of turgor loss point (TLP), and the 50% losses of stomatal conductance $g_{s\,50}$, leaf hydraulic conductance $K_{leaf\,50}$, and rehydration capacity PLRC$_{50}$ averaged for the four measured species. ns, nonsignificant differences between the mean values of each index under different irradiances (paired t-test across species; $P \leq 0.05$).

$P = 0.003$), Ψ_{leaf} at $K_{leaf\,50,80}$ and $K_{x\,50,88}$ (Table S9), and Ψ_{TLP} with several Ψ_{leaf} thresholds for dehydration responses, including those of PLRC, K_{leaf}, K_{ox}, and K_x (Table S9).

Discussion

By analyzing measurements of dehydration impacts on mesophyll, hydraulic, and stomatal functions of a set of diverse angiosperm species, our study provides a thorough sequence of water status thresholds driving leaf functional decline (Fig. 8). We show for the first time that leaf damage as shown by loss of rehydration and light-harvesting capacities occur with dehydration beyond severe failure of hydraulic function. Further, we show an association of rehydration capacity decline with drought sensitivity traits such as TLP and leaf hydraulic vulnerability. Species showed much stronger variability and diversification in Ψ_{leaf} thresholds than RWC did.

Leaf rehydration capacity, a potential indicator of drought tolerance

We found strong decline in rehydration capacity during dehydration. The decline of rehydration capacity with RWC was best described by a sigmoid function for most species, suggesting that leaf rehydration capacity is unaffected at mild dehydration levels. A first stable phase was followed by an abrupt decrease in rehydration capacity, which would result from irreversible loss of cell volume or the death of cells. The second stable phase, which occurs at very low RWCs, may represent apoplastic water intake by capillarity, which would be independent of the dysfunction of the parenchyma mesophyll tissue. Rehydration surveys in excised and intact *Laurus nobilis* plants using X-ray microtomography found water refilling of the xylem and apoplast by capillary forces in excised samples, but seldom in intact plants (Knipfer *et al.*, 2017). An avenue for future research is the development of methods to quantify leaf PLRC under *in vivo* conditions to verify the rehydration dynamics shown by rehydration curves and the mechanisms involved in the loss of rehydration capacity.

Thresholds of F_v/F_m decline and its lack of post-dehydration recovery

Water content decline had a strong impact on the maximum quantum yield of fluorescence. Most species showed an exponential decrease of F_v/F_m during dehydration, with a rapid drop *c.* 20% RWC, suggesting significant damage late in dehydration stress. This finding is consistent with a previous study on *Arabidopsis*, which showed declines of F_v/F_m at a very similar RWC threshold (Woo *et al.*, 2008). Several previous studies have suggested that leaf photochemistry is relatively stable under water stress (Shabala & Pang, 2007; Flexas *et al.*, 2009), as declines in PSII photochemistry occur at lower water contents than g_s and TLP (Boyer & Potter, 1973; Miyashita *et al.*, 2005). Moreover, significant declines in F_v/F_m occur after the complete loss of midrib xylem hydraulic function in sunflower plants (Cardoso *et al.*, 2018). We importantly extended these findings showing

Fig. 5 Leaf functional impairment over a gradient of decreasing total relative water content. Red bars are mean values for each threshold. Boxes show the 25th and 75th percentiles, and bars indicate extreme values. Colors illustrate different thresholds of leaf conductance (K_{leaf}, K_x, K_{ox}; blue), stomatal conductance (g_s; yellow), turgor loss point (TLP; orange), loss of rehydration capacity (PLRC; green), and loss of F_v/F_m (PLCF; purple). Numbers next to each threshold are percentages of function loss. K_{leaf}, K_{ox}, K_x, and TLP values were obtained from Scoffoni et al. (2011, 2017), Guyot et al. (2012), and Bartlett et al. (2012b). Values for each measured threshold are provided in Table 2 and Supporting Information Table S10. Pairwise independent t-test comparisons between all of the thresholds included in this sequence are available in Table S6.
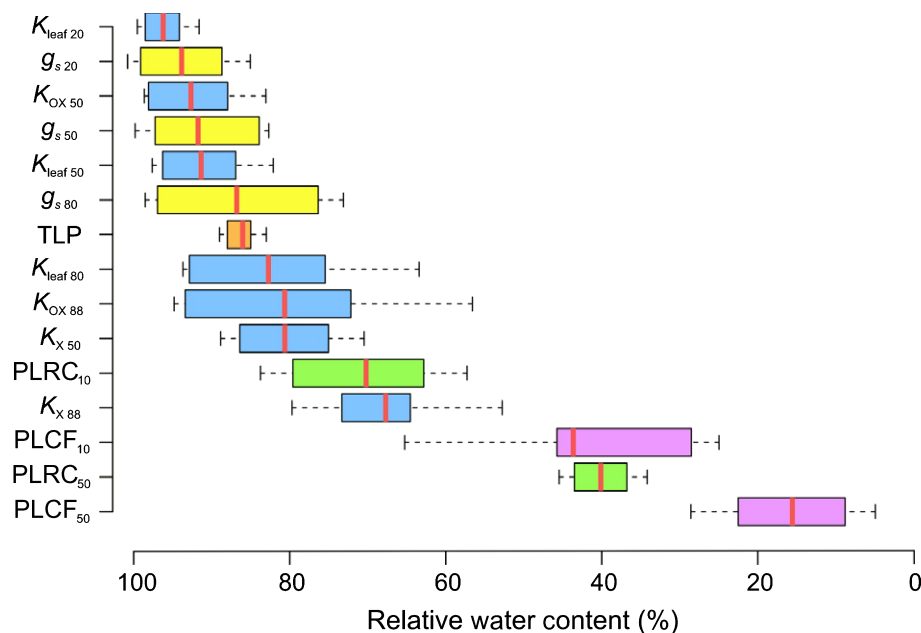

Fig. 6 Leaf functional impairment over a gradient of decreasing water potential. Red bars are mean values for each threshold. Boxes show the 25th and 75th percentiles, and bars indicate minimum and maximum values. Colors illustrate different thresholds of leaf conductance (K_{leaf}, K_x, K_{ox}; blue), stomatal conductance (g_s; yellow), turgor loss point (TLP; orange), and loss of rehydration capacity (PLRC; green). Numbers next to each threshold are percentages of function loss. K_{leaf}, K_{ox}, K_x, and TLP values were obtained from Scoffoni et al. (2011, 2017), Guyot et al. (2012), and Bartlett et al. (2012b). Values for each threshold are provided in Supporting Information Table S11. Pairwise independent t-test comparisons between all of the thresholds included in this sequence are available in Table S7.
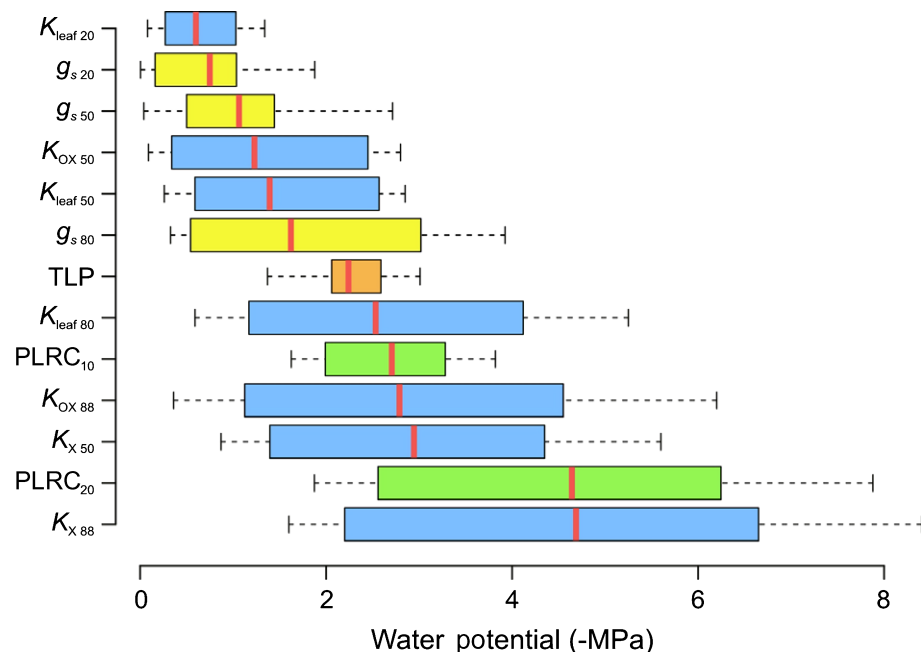
that photochemical damage is reached only after full hydraulic disruption in a range of diverse species. The F_v/F_m declines occur at extremely low RWC and Ψ_{leaf}, demonstrating that the light-harvesting function of the leaf is compromised at much lower water status than those triggering substantial loss of hydraulic function. Indeed, PSII maximum quantum yield was the last function to decrease in the sequence of dehydration-induced damage. Notably, desiccation-tolerant plants, also known as 'resurrection' plants, show similar rapid declines of F_v/F_m when reaching RWC of c. 20% (Beckett et al., 2012; Zia et al., 2016), suggesting a common dehydration threshold for major photochemistry damage even for species with photosynthetic repair capabilities.

Our experiments on the 10 species focused on F_v/F_m in the ambient light of the laboratory specifically to isolate the effect of dehydration on leaf photochemistry without excess light and temperature stresses. We note that high irradiance can induce faster photoinhibition, ultimately leading to greater photochemical damage (Björkman, 1987). Indeed, our measurements on a subset of four species showed an empirical, nonsignificant tendency for photochemistry dysfunction to occur earlier when leaves were dehydrated under high irradiance. However, even under high irradiance, F_v/F_m declines are known to occur at very strong levels of water stress (Flexas et al., 2009). Our experiments confirmed that photochemical decline in leaves dehydrated under low or high irradiance occurs after major hydraulic dysfunction.

Further, when K_{leaf} and g_s declines are considered under low irradiance, they show lower maximum values, and lower sensitivity to dehydration (Guyot *et al.*, 2012). Thus, the sequence of impacts of leaf dehydration is expected to be maintained under different light irradiances. We observed no recovery of F_v/F_m after rehydration, suggesting irreversible impairment of photochemical activity as previously shown in crops undergoing various levels of water stress (Giardi *et al.*, 1996; Souza *et al.*, 2004). Dehydration-induced photochemical decline, and its lack of recovery, may result from injuries to thylakoid membranes or proteins (Hincha *et al.*, 1987; Tambussi *et al.*, 2000; Hoekstra *et al.*, 2001; Sharkey, 2005). We tested whether the decrease in F_v/F_m might be associated with Chl degradation associated with dark-induced senescence (Hörtensteiner, 2006), as previously reported for excised barley leaves maintained well hydrated in darkness (Scheumann *et al.*, 1999). However, our measurements showed that total Chl concentration was maintained in our experimental dehydration treatment. In addition to its effect on photochemistry, water scarcity primarily affects photosynthesis by reducing CO_2 diffusion to the chloroplast due to declines of stomatal and mesophyll conductance (Flexas *et al.*, 2008), with possible additional impacts on carbon reaction biochemistry (Tezara *et al.*, 1999; Grassi & Magnani, 2005). Future work is needed to clarify the impacts of dehydration on the entire photosynthetic system in relation to the leaf stomatal, hydraulic, wilting, and damage thresholds included in this study.

Table 3 Ranges and variation of drought tolerance thresholds.

Index	RWC CV (%)	RWC range min/max (%)	Ψ CV (%)	Ψ range min/max (−MPa)	SLRT statistic (P-value)
$K_{leaf\ 20}$	2.9	92/99	78.1	1.34/0.08	232***
$g_{s\ 20}$	6.2	85/>99	88.8	1.88/0.01	228***
$K_{ox\ 50}$	6.4	83/98	92.5	2.80/0.09	225***
$g_{s\ 50}$	7.6	83/>99	83.6	2.72/0.04	230***
$K_{leaf\ 50}$	6.5	82/98	78.5	2.85/0.26	232***
$g_{s\ 80}$	12.1	73/98	80.9	3.93/0.33	225***
TLP	3.9	78/89	30.3	3.45/1.18	224***
$K_{leaf\ 80}$	12.9	63/94	67.8	5.25/0.59	222***
$K_{ox\ 88}$	16.9	57/95	75.2	6.20/0.36	229***
$K_{x\ 50}$	8.5	70/89	61.5	5.60/0.87	226***
$PLRC_{10}$	14.3	57/84	32.4	3.82/1.63	229***
$K_{x\ 88}$	12.3	53/80	53.7	8.40/1.60	221***
$PLCF_{10}$	53.4	25/99	na	na	na
$PLRC_{50}$	9.9	34/45	na	na	na
$PLCF_{50}$	52.4	5/29	na	na	na

Coefficients of variation (CVs) and range of values of relative water content (RWC) and water potential (Ψ_{leaf}) thresholds of functional decline. Thresholds are ordered from highest to least sensitive in terms of RWC mean values. Note that high sensitivity in some thresholds was found due to estimation of Ψ_{leaf} thresholds using maximum likelihood statistical functions and extrapolating high maximum values for stomatal conductance and hydraulic conductance for fully hydrated leaves ($\Psi_{leaf} = 0$ MPa), and RWC thresholds were estimated from Ψ_{leaf} thresholds using pressure–volume curves (see the Materials and Methods section). See Table 1 for a list of abbreviations and units. na, not available, lack of Ψ_{leaf} thresholds. SLRT, signed-likelihood ratio test for equality of CVs. ***, $P \leq 0.001$.

Correlations among thresholds of dehydration-induced leaf functional decline

We observed significant intercorrelation of most drought-tolerance thresholds across species. This finding supports the hypothesis for the coordination among thresholds proposed in a meta-analysis of a smaller set of responses (Bartlett *et al.*, 2016), and extends this coordination to many more leaf drought-tolerance traits. Such correlations among the thresholds for functional declines with dehydration would represent co-selection for drought tolerance, or mechanistic trait linkages. For instance, we observed correlations of $RWC_{PLRC_{50}}$ with all the RWC thresholds of leaf hydraulic conductance ($RWC_{K_{leaf}}$), and outside-xylem hydraulic conductance ($RWC_{K_{ox}}$). The relationship of thresholds for declines in K_{ox} and rehydration capacity is consistent with the extra-xylary pathways representing a locus for the control of water relations during dehydration, influenced by aquaporins that
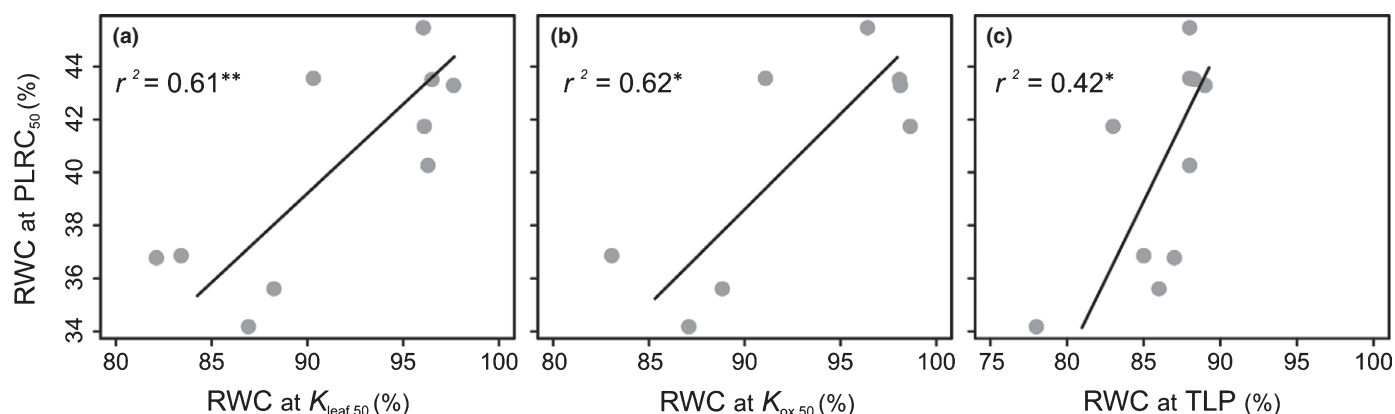

Fig. 7 Relationships of the relative water content (RWC) inducing 50% loss of rehydration capacity with RWC thresholds of decline in leaf hydraulic conductance (a), outside-xylem hydraulic conductance (b), and leaf turgor loss point (TLP) (c) across species. Values of decline in outside-xylem hydraulic conductance were available only for eight of the species studied. K_{leaf}, K_{ox} and TLP values were obtained from Scoffoni *et al.* (2011, 2017), Guyot *et al.* (2012), and Bartlett *et al.* (2012b). Standardized major axes regressions are included. *, $P \leq 0.05$; **, $P \leq 0.01$.

Table 4 Correlations of the relative water content (RWC) indices of loss of rehydration capacity and Chl fluorescence (F_v/F_m) with other RWC indices of leaf functional impairment.

	RWC_{TLP}	$RWC_{K_{10}}$	$RWC_{K_{20}}$	$RWC_{K_{50}}$	$RWC_{K_{80}}$	$RWC_{K_{ox\,50}}$	$RWC_{K_{ox\,88}}$	$RWC_{K_{x\,50}}$	$RWC_{K_{x\,88}}$	$RWC_{g_{s\,20}}$	$RWC_{g_{s\,50}}$	$RWC_{g_{s\,80}}$
$RWC_{PLRC_{10}}$	0.53	0.59	0.62	0.57	0.48	**0.72***	0.59	0	0.09	0.51	0.58	0.55
$RWC_{PLRC_{20}}$	0.57	**0.64***	**0.66***	0.61	0.52	**0.72***	0.6	−0.02	0.15	0.5	0.58	0.58
$RWC_{PLRC_{50}}$	**0.65***	**0.80****	**0.80****	**0.78****	**0.75***	**0.79***	**0.84****	0.1	0.26	0.33	0.43	0.54
$RWC_{PLCF_{10}}$	0.37	0.19	0.10	0.07	−0.03	0.01	−0.03	−0.22	0.26	0.31	0.3	0.3
$RWC_{PLCF_{20}}$	0.44	0.27	0.18	0.12	−0.01	0.07	−0.01	−0.37	0.2	0.46	0.46	0.42
$RWC_{PLCF_{50}}$	0.51	0.46	0.41	0.28	0.13	0.27	0.11	−0.69	−0.06	**0.77****	**0.8****	**0.64***

Pearson's correlation coefficients of bivariate cross-correlations. Bold values indicate significant correlations. $n = 10$ for all variables, except K_{ox} and K_x indices, for which $n = 8$. See Table 1 for a list of abbreviations and units. See Supporting Information Tables S8 and S9 for a full correlation matrix amongst RWC and Ψ_{leaf} thresholds of functional decline.

*, $P \leq 0.05$; **, $P \leq 0.01$.

would modulate the flow of water during transpiration and also during cell rehydration (Scoffoni *et al.*, 2017). Further, we observed a correlation of $RWC_{PLRC_{50}}$ and $\Psi_{PLRC_{10}}$ with RWC_{TLP} and Ψ_{TLP}, respectively. These correlations may arise from the impact of turgor loss in the mesophyll and more specifically on the outside-xylem hydraulic pathway (Scoffoni *et al.*, 2014), which would constrain leaf rehydration capacity. We also observed a relationship across species between leaf hydraulic declines and $\Psi_{PLRC_{10}}$. This relationship is consistent with previous studies that emphasized the importance of leaf hydraulic failure in limiting functional recovery after rewatering (Brodribb & Cochard, 2009; Skelton *et al.*, 2017b). However, this correlation may also be driven by a trait co-selection exerted by water stress on both traits for dehydration tolerance and resilience. We found a strong association of the RWC inducing a 50% decline of F_v/F_m, with the thresholds of g_s decline across the species studied, indicating that different tissues are integrated in their tolerance of dehydration (chloroplasts in the mesophyll and guard cells in the epidermis).

Thresholds for functional decline during dehydration in leaf relative water content vs leaf water potential

All the measured dehydration tolerance thresholds showed less variability in terms of RWC than of Ψ_{leaf}. A previous study reported narrower variability in stomatal conductance responses to RWC than in Ψ_{leaf} for soybean (*Glycine max*) and maize (*Zea mays*) (Bennett *et al.*, 1987). A narrow variability in RWC thresholds may represent convergence in the hydration levels necessary to protect mesophyll cells, and ultimately the chloroplasts, from loss of function and damage. Despite the advantages of Ψ_{leaf} for the plant physiologist (e.g. the typically higher precision of Ψ_{leaf} measurement, and its direct representation of the driving forces for water movement), RWC can be a valuable water status indicator of cell stress, as it represents relative cell volume shrinkage, and thus tension on the cell and vacuolar membranes, cytoskeleton and cell wall and cell solute concentrations (Sack *et al.*, 2018). Our study illustrates how different water status indices should be considered in plant–water relations studies and especially assessed for their value as proxies for dehydration-induced responses.

The sequence of dehydration-induced functional decline

We provided an empirically based sequence of functional and structural damage in response to leaf water stress. Our sequence of Ψ_{leaf} thresholds is similar for the three traits in common with those considered in the meta-analysis of Bartlett *et al.* (2016); that is, $g_{s\,50}$, $K_{leaf\,50}$, and TLP occur sequentially as leaves dehydrate. Notably, the water status thresholds for 50% declines in g_s and K_{leaf} were not significantly different, consistent with coordination on average between leaf hydraulic decline (which depends strongly on the outside-xylem pathways) and stomatal closure (Brodribb & Holbrook, 2003; Scoffoni & Sack, 2017). During leaf dehydration, $g_{s\,50}$ occurred significantly before the declines in leaf xylem conductance $K_{x\,50}$, consistent with recent reports of stomatal closure preceding the appearance of embolism in grapevines (Hochberg *et al.*, 2017). On average across species, $RWC_{g_{s\,80}}$ occurred at similar water status as RWC_{TLP} (87% ± 3.31 vs 86% ± 1.05, respectively; Table S6), consistent with mild cell dehydration as a driver of ABA accumulation and stomatal closure (McAdam & Brodribb, 2016; Sack *et al.*, 2018). The sequential occurrence of $g_{s\,80}$ and TLP suggests that significant stomatal closure may act to prevent mesophyll damage.

On average across species, $PLRC_{10}$ occurred at lower RWC and Ψ_{leaf} than TLP did, and at similar water status to $K_{x\,88}$, which represents major vein xylem embolism (Scoffoni *et al.*, 2016) and which, for stem xylem, has been proposed as a hydraulic threshold indicating irreversible drought damage (Urli *et al.*, 2013). Notably, $PLRC_{10}$, along with the majority of the hydraulic traits included in the sequence, occurred at thresholds less negative than the −4 MPa maximal boundary of absolute stomatal closure (Martin-StPaul *et al.*, 2017). $PLRC_{50}$ occurred at significantly lower water status, demonstrating that partial leaf rehydration capacity exists even beyond significant mesophyll damage and hydraulic dysfunction.

The sequence established in this study of 10 diverse angiosperm species indicates an 'outside to inside' progression of overall leaf sensitivity to dehydration through the leaf tissues and cells. Stomatal closure and outside-xylem hydraulic decline tend to begin with mild dehydration and to peak at around TLP, with xylem embolism occurring later, followed by substantial
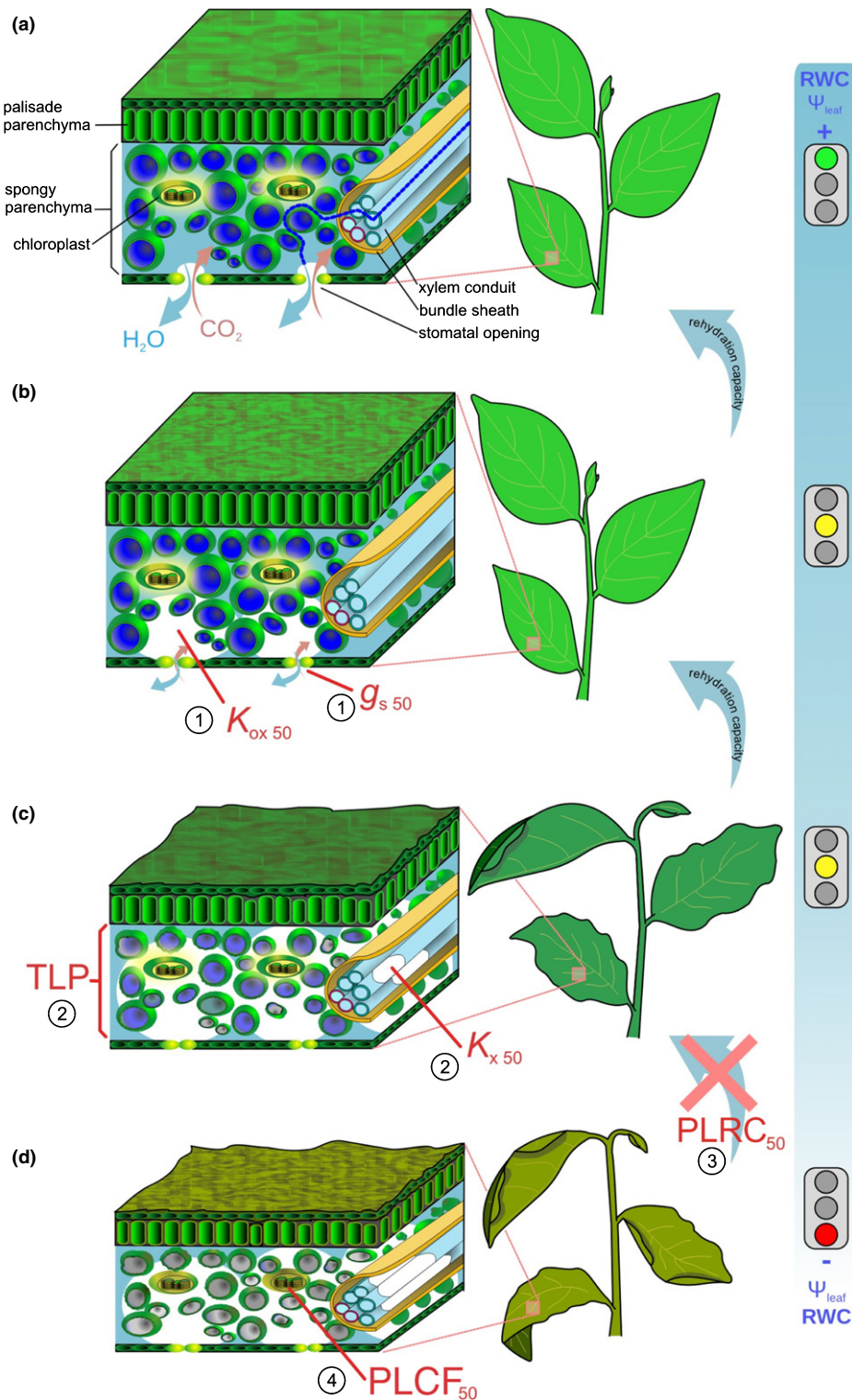
Fig. 8 Thresholds of dysfunction at different stages of leaf dehydration. (a) Fully operational leaf with a continual water flow through the leaf vein xylem conduits, bundle sheath, and spongy parenchyma (blue dashed line). (b) A 50% decrease of outside-xylem and stomatal conductance. (c) Occurrence of vein xylem embolism inducing a 50% decrease of xylem-specific conductance, and loss of turgor inducing significant changes in leaf thickness and damage to mesophyll cells. At this stage, there is a strong reduction of the stomatal aperture, severely diminishing stomatal conductance. TLP, turgor loss point. (d) Severe dehydration inducing disruption of the hydraulic function, major damage in mesophyll cells, loss of rehydration capacity, and a decreased photochemical activity in the chloroplast. PLCF, percentage loss of Chl fluorescence. Thresholds occurrences are marked by red letters. Circled numbers indicate the order of occurrence of each dehydration-induced impact on leaf function. Symbols and definitions of thresholds are provided in Table 1. Relative water content (RWC) and Ψ_{leaf} thresholds of functional loss and analyses of sequence occurrences are provided in the Supporting Information.

irrecoverable damage, as indicated by loss of rehydration capacity, and, finally, irreversible damage to the photochemical system in the chloroplast (Fig. 8). Species with greater overall drought tolerance show shifts of multiple elements of the system to better resist declines during dehydration. Notably, by the time that substantial damage has occurred to the leaves, many functions have declined, and so estimating the early impacts of drought on water balance or photosynthesis should focus on hydraulic traits rather than photodamage. A distinction between 'dehydration' and 'desiccation' has been proposed to occur at a RWC of 30–40% based on the initiation of major physiological and molecular changes (Zhang & Bartels, 2018), and most extant angiosperms cannot survive the dehydration of their vegetative tissues to 20–30% RWC (Oliver *et al.*, 2010). Our findings show that major physiological processes decline in the dehydration stage, as for the 10 study species we observed a major decrease of hydraulic functions before 40% RWC, and only F_v/F_m function persisted below the 40% boundary. Given that declines in F_v/F_m seem to occur at the very end of the dehydration-induced injury sequence, our study suggests that the functions of the PSII are maintained beyond the point at which photosynthetic CO_2 assimilation and hydraulic functioning are impaired.

Our findings provide a baseline sequence for the declines of functions to be confirmed in larger comparisons of plant species and functional types. Further, these observations should be considered in studies relying on decline in chloroplast function as an indicator of drought effects at the leaf scale when ChlF is used as an indicator of drought impact, since declines in ChlF occur at the late stages of water stress (Yao *et al.*, 2018). Based on our findings, such declines of leaf photochemistry performance would correspond to irreversible damage to leaf functionality, beyond stomatal closure, leaf vein embolism, and irreversible loss of rehydration capacity.

Author contributions

ST and LS designed the research. RP performed measurements of stomatal conductance. CS contributed data of leaf hydraulic vulnerability. SDD and GPJ contributed to the design of measurement protocols. ST performed experiments, analyzed the data, and wrote the first draft of the manuscript with contributions from LS. All authors contributed to subsequent revisions of the manuscript.

ORCID

Grace P. John https://orcid.org/0000-0002-8045-5982
Lawren Sack https://orcid.org/0000-0002-7009-7202
Christine Scoffoni https://orcid.org/0000-0002-2680-3608
Santiago Trueba https://orcid.org/0000-0001-8218-957X

References

Adams HD, Zeppel MJ, Anderegg WR, Hartmann H, Landhäusser SM, Tissue DT, Huxman TE, Hudson PJ, Franz TE, Allen CD *et al.* 2017. A multi-species synthesis of physiological mechanisms in drought-induced tree mortality. *Nature Ecology & Evolution* 1: 1285–1291.

Allen CD, Breshears DD, Mcdowell NG. 2015. On underestimation of global vulnerability to tree mortality and forest die-off from hotter drought in the Anthropocene. *Ecosphere* 6: art129.

Allen CD, Macalady AK, Chenchouni H, Bachelet D, Mcdowell N, Vennetier M, Kitzberger T, Rigling A, Breshears DD, Hogg ET *et al.* 2010. A global overview of drought and heat-induced tree mortality reveals emerging climate change risks for forests. *Forest Ecology and Management* 259: 660–684.

Anderegg WRL, Wolf A, Arango-Velez A, Choat B, Chmura DJ, Jansen S, Kolb T, Li S, Meinzer F, Pita P *et al.* 2017. Plant water potential improves prediction of empirical stomatal models. *PLoS ONE* 12: e0185481.

Arndt SK, Irawan A, Sanders GJ. 2015. Apoplastic water fraction and rehydration techniques introduce significant errors in measurements of relative water content and osmotic potential in plant leaves. *Physiologia Plantarum* 155: 355–368.

Asner GP, Brodrick PG, Anderson CB, Vaughn N, Knapp DE, Martin RE. 2016. Progressive forest canopy water loss during the 2012–2015 California drought. *Proceedings of the National Academy of Sciences, USA* 113: E249–E255.

Baker NR. 2008. Chlorophyll fluorescence: a probe of photosynthesis *in vivo*. *Annual Review of Plant Biology* 59: 89–113.

Bartlett MK, Klein T, Jansen S, Choat B, Sack L. 2016. The correlations and sequence of plant stomatal, hydraulic, and wilting responses to drought. *Proceedings of the National Academy of Sciences, USA* 113: 13098–13103.

Bartlett MK, Scoffoni C, Ardy R, Zhang Y, Sun S, Cao K, Sack L. 2012b. Rapid determination of comparative drought tolerance traits: using an osmometer to predict turgor loss point. *Methods in Ecology and Evolution* 3: 880–888.

Bartlett MK, Scoffoni C, Sack L. 2012a. The determinants of leaf turgor loss point and prediction of drought tolerance of species and biomes: a global meta-analysis. *Ecology Letters* 15: 393–405.

Bates D, Mächler M, Bolker B, Walker S. 2014. Fitting linear mixed-effects models using LME4. *Journal of Statistical Software* 67: 1–51.

Beckett M, Loreto F, Velikova V, Brunetti C, Di Ferdinando M, Tattini M, Calfapietra C, Farrant JM. 2012. Photosynthetic limitations and volatile and non-volatile isoprenoids in the poikilochlorophyllous resurrection plant *Xerophyta humilis* during dehydration and rehydration. *Plant, Cell & Environment* 35: 2061–2074.

Bennett JM, Sinclair TR, Muchow RC, Costello SR. 1987. Dependence of stomatal conductance on leaf water potential, turgor potential, and relative water content in field-grown soybean and maize. *Crop Science* 27: 984–990.

Björkman O. 1987. High-irradiance stress in higher plants and interaction with other stress factors. In: Biggins J, ed. *Progress in photosynthesis research: Volume 4 Proceedings of the VIIth International Congress on Photosynthesis, Providence, Rhode Island, USA, 10–15 August 1986.* Dordrecht, the Netherlands: Springer, 11–18.

Blackman CJ, Brodribb TJ, Jordan GJ. 2009. Leaf hydraulics and drought stress: response, recovery and survivorship in four woody temperate plant species. *Plant, Cell & Environment* 32: 1584–1595.

Boyer JS, Potter JR. 1973. Chloroplast response to low leaf water potentials: I. Role of turgor. *Plant Physiology* 51: 989–992.

Breshears DD, Cobb NS, Rich PM, Price KP, Allen CD, Balice RG, Romme WH, Kastens JH, Floyd ML, Belnap J *et al.* 2005. Regional vegetation die-off

in response to global-change-type drought. *Proceedings of the National Academy of Sciences, USA* 102: 15144–15148.

Brodribb TJ, Cochard H. 2009. Hydraulic failure defines the recovery and point of death in water-stressed conifers. *Plant Physiology* 149: 575–584.

Brodribb TJ, Holbrook NM. 2003. Stomatal closure during leaf dehydration, correlation with other leaf physiological traits. *Plant Physiology* 132: 2166–2173.

Brodribb TJ, Holbrook NM. 2006. Declining hydraulic efficiency as transpiring leaves desiccate: two types of response. *Plant, Cell & Environment* 29: 2205–2215.

Brodribb TJ, McAdam SA. 2011. Passive origins of stomatal control in vascular plants. *Science* 331: 582.

Burnham KP, Anderson DR. 2003. *Model selection and multimodel inference: a practical information-theoretic approach.* New York, NY, USA: Springer Science & Business Media.

Cai Y, Wang J, Li S, Zhang L, Peng L, Xie W, Liu F. 2015. Photosynthetic response of an alpine plant, *Rhododendron delavayi* Franch, to water stress and recovery: the role of mesophyll conductance. *Frontiers in Plant Science* 6: e1089.

Cardoso AA, Brodribb TJ, Lucani CJ, Damatta FM, McAdam SAM. 2018. Coordinated plasticity maintains hydraulic safety in sunflower leaves. *Plant, Cell & Environment* 41: 2567–2576.

Flexas J, Barón M, Bota J, Ducruet J-M, Gallé A, Galmés J, Jiménez M, Pou A, Ribas-Carbó M, Sajnani C *et al.* 2009. Photosynthesis limitations during water stress acclimation and recovery in the drought-adapted *Vitis* hybrid Richter-110 (*V. berlandieri*× *V. rupestris*). *Journal of Experimental Botany* 60: 2361–2377.

Flexas J, Ribas-Carbó M, Diaz-Espejo A, Galmés J, Medrano H. 2008. Mesophyll conductance to CO_2: current knowledge and future prospects. *Plant, Cell & Environment* 31: 602–621.

Galmés J, Medrano H, Flexas J. 2007. Photosynthetic limitations in response to water stress and recovery in Mediterranean plants with different growth forms. *New Phytologist* 175: 81–93.

Genty B, Briantais J-M, Baker NR. 1989. The relationship between the quantum yield of photosynthetic electron transport and quenching of chlorophyll fluorescence. *Biochimica et Biophysica Acta (BBA) - General Subjects* 990: 87–92.

Genty B, Briantais J-M, Da Silva JBV. 1987. Effects of drought on primary photosynthetic processes of cotton leaves. *Plant Physiology* 83: 360.

Giardi MT, Cona A, Geiken B, Kuèera T, Masojídek J, Mattoo AK. 1996. Long-term drought stress induces structural and functional reorganization of photosystem II. *Planta* 199: 118–125.

Grassi G, Magnani F. 2005. Stomatal, mesophyll conductance and biochemical limitations to photosynthesis as affected by drought and leaf ontogeny in ash and oak trees. *Plant, Cell & Environment* 28: 834–849.

Guadagno CR, Ewers BE, Speckman HN, Aston TL, Huhn BJ, Devore SB, Ladwig JT, Strawn RN, Weinig C. 2017. Dead or alive? Using membrane failure and chlorophyll fluorescence to predict mortality from drought. *Plant Physiology* 175: 223–234.

Guyot G, Scoffoni C, Sack L. 2012. Combined impacts of irradiance and dehydration on leaf hydraulic conductance: insights into vulnerability and stomatal control. *Plant, Cell & Environment* 35: 857–871.

Hincha DK, Höfner R, Schwab KB, Heber U, Schmitt JM. 1987. Membrane rupture is the common cause of damage to chloroplast membranes in leaves injured by freezing or excessive wilting. *Plant Physiology* 83: 251–253.

Hochberg U, Windt CW, Ponomarenko A, Zhang Y-J, Gersony J, Rockwell FE, Holbrook NM. 2017. Stomatal closure, basal leaf embolism and shedding protect the hydraulic integrity of grape stems. *Plant Physiology* 174: 764–775.

Hoekstra FA, Golovina EA, Buitink J. 2001. Mechanisms of plant desiccation tolerance. *Trends in Plant Science* 6: 431–438.

Hörtensteiner S. 2006. Chlorophyll degradation during senescence. *Annual Review of Plant Biology* 57: 55–77.

John GP, Henry C, Sack L. 2018. Leaf rehydration capacity: associations with other indices of drought tolerance and environment. *Plant, Cell & Environment* 41: 2638–2653.

Klein T. 2014. The variability of stomatal sensitivity to leaf water potential across tree species indicates a continuum between isohydric and anisohydric behaviours. *Functional Ecology* 28: 1313–1320.

Knipfer T, Cuneo IF, Earles JM, Reyes C, Brodersen CR, Mcelrone AJ. 2017. Storage compartments for capillary water rarely refill in an intact woody plant. *Plant Physiology* 175: 1649.

Krishnamoorthy K, Lee M. 2014. Improved tests for the equality of normal coefficients of variation. *Computational Statistics* 29: 215–232.

Kuznetsova A, Brockhoff PB, Christensen RHB. 2017. LMERTEST package: tests in linear mixed effects models. *Journal of Statistical Software* 82: 1–26.

Lawlor DW, Cornic G. 2002. Photosynthetic carbon assimilation and associated metabolism in relation to water deficits in higher plants. *Plant, Cell & Environment* 25: 275–294.

Li S, Feifel M, Karimi Z, Schuldt B, Choat B, Jansen S. 2016. Leaf gas exchange performance and the lethal water potential of five European species during drought. *Tree Physiology* 36: 179–192.

Martin-StPaul N, Delzon S, Cochard H. 2017. Plant resistance to drought depends on timely stomatal closure. *Ecology Letters* 20: 1437–1447.

Martorell S, Diaz-Espejo A, Medrano H, Ball MC, Choat B. 2014. Rapid hydraulic recovery in *Eucalyptus pauciflora* after drought: linkages between stem hydraulics and leaf gas exchange. *Plant, Cell & Environment* 37: 617–626.

Marwick B, Krishnamoorthy K. 2016. *CVEQUALITY: tests for the equality of coefficients of variation from multiple groups. R package version 0.1.1.* [WWW document] URL https://CRAN.R-project.org/package=cvequality [accessed November 2017].

McAdam SaM, Brodribb TJ. 2016. Linking turgor with ABA biosynthesis: implications for stomatal responses to vapour pressure deficit across land plants. *Plant Physiology* 171: 2008–2016.

Meinzer FC, Johnson DM, Lachenbruch B, Mcculloh KA, Woodruff DR. 2009. Xylem hydraulic safety margins in woody plants: coordination of stomatal control of xylem tension with hydraulic capacitance. *Functional Ecology* 23: 922–930.

Miyashita K, Tanakamaru S, Maitani T, Kimura K. 2005. Recovery responses of photosynthesis, transpiration, and stomatal conductance in kidney bean following drought stress. *Environmental and Experimental Botany* 53: 205–214.

Murchie EH, Lawson T. 2013. Chlorophyll fluorescence analysis: a guide to good practice and understanding some new applications. *Journal of Experimental Botany* 64: 3983–3998.

Nardini A, Luglio J. 2014. Leaf hydraulic capacity and drought vulnerability: possible trade-offs and correlations with climate across three major biomes. *Functional Ecology* 28: 810–818.

Oliver MJ, Cushman JC, Koster KL. 2010. Dehydration tolerance in plants. In: Sunkar R, ed. *Plant stress tolerance: methods and protocols.* Totowa, NJ, USA: Humana Press, 3–24.

Oppenheimer HR. 1963. Zur Kenntnis kritischer Wasser-Sättigungsdefizite in Blättern und ihrer Bestimmung. *Planta* 60: 51–69.

Oppenheimer HR, Leshem B. 1966. Critical thresholds of dehydration in leaves of *Nerium oleander* L. *Protoplasma* 61: 302–321.

Pasquet-Kok J, Creese C, Sack L. 2010. Turning over a new 'leaf': multiple functional significances of leaves versus phyllodes in Hawaiian *Acacia koa.* *Plant, Cell & Environment* 33: 2084–2100.

R Core Team. 2017. *R: a language and environment for statistical computing.* Vienna, Austria: R Foundation for Statistical Computing.

Sack L, John GP, Buckley TN. 2018. ABA accumulation in dehydrating leaves is associated with decline in cell volume, not turgor pressure. *Plant Physiology* 176: 489.

Sack L, Pasquet-Kok J, Prometheuswiki Contributors. 2011. *Leaf pressure–volume curve parameters.* [WWW document] URL http://prometheuswiki.org/tiki-index.php?page=Leaf%20pressure-volume%20curve%20parameters [accessed 16 November 2017].

Scheumann V, Schoch S, Rüdiger W. 1999. Chlorophyll *b* reduction during senescence of barley seedlings. *Planta* 209: 364–370.

Scoffoni C, Albuquerque C, Brodersen C, Townes SV, John GP, Bartlett MK, Buckley TN, McElrone AJ, Sack L. 2017. Outside-xylem vulnerability, not xylem embolism, controls leaf hydraulic decline during dehydration. *Plant Physiology* 173: 1197–1210.

Scoffoni C, Albuquerque C, Brodersen CR, Townes SV, John GP, Cochard H, Buckley TN, McElrone AJ, Sack L. 2016. Leaf vein xylem conduit diameter influences susceptibility to embolism and hydraulic decline. *New Phytologist* 213: 1076–1092.

Scoffoni C, Rawls M, Mckown A, Cochard H, Sack L. 2011. Decline of leaf hydraulic conductance with dehydration: relationship to leaf size and venation architecture. *Plant Physiology* 156: 832–843.

Scoffoni C, Sack L. 2017. The causes and consequences of leaf hydraulic decline with dehydration. *Journal of Experimental Botany* 68: 4479–4496.

Scoffoni C, Vuong C, Diep S, Cochard H, Sack L. 2014. Leaf shrinkage with dehydration: coordination with hydraulic vulnerability and drought tolerance. *Plant Physiology* 164: 1772–1788.

Shabala S, Pang J. 2007. Chlorophyl fluorescence as a screening tool in plant breeding. In: Hemantaranjan A, ed. *Environmental physiology*. Jodhpur, India: Pawan Kumar Scientific Publishers, 95–184.

Sharkey TD. 2005. Effects of moderate heat stress on photosynthesis: importance of thylakoid reactions, Rubisco deactivation, reactive oxygen species, and thermotolerance provided by isoprene. *Plant, Cell & Environment* 28: 269–277.

Sinclair TR, Ludlow MM. 1985. Who taught plants thermodynamics? The unfulfilled potential of plant water potential. *Functional Plant Biology* 12: 213–217.

Skelton RP, Brodribb TJ, Choat B. 2017a. Casting light on xylem vulnerability in an herbaceous species reveals a lack of segmentation. *New Phytologist* 214: 561–569.

Skelton RP, Brodribb TJ, McAdam SaM, Mitchell PJ. 2017b. Gas exchange recovery following natural drought is rapid unless limited by loss of leaf hydraulic conductance: evidence from an evergreen woodland. *New Phytologist* 215: 1399–1412.

Souza RP, Machado EC, Silva JaB, Lagôa AMMA, Silveira JaG. 2004. Photosynthetic gas exchange, chlorophyll fluorescence and some associated metabolic changes in cowpea (*Vigna unguiculata*) during water stress and recovery. *Environmental and Experimental Botany* 51: 45–56.

Tambussi EA, Bartoli CG, Beltrano J, Guiamet JJ, Araus JL. 2000. Oxidative damage to thylakoid proteins in water-stressed leaves of wheat (*Triticum aestivum*). *Physiologia Plantarum* 108: 398–404.

Tezara W, Mitchell VJ, Driscoll SD, Lawlor DW. 1999. Water stress inhibits plant photosynthesis by decreasing coupling factor and ATP. *Nature* 401: 914.

Trenberth KE, Dai A, Van Der Schrier G, Jones PD, Barichivich J, Briffa KR, Sheffield J. 2014. Global warming and changes in drought. *Nature Climate Change* 4: 17–22.

Uddling J, Gelang-Alfredsson J, Piikki K, Pleijel H. 2007. Evaluating the relationship between leaf chlorophyll concentration and SPAD-502 chlorophyll meter readings. *Photosynthesis Research* 91: 37–46.

Urli M, Porté AJ, Cochard H, Guengant Y, Burlett R, Delzon S. 2013. Xylem embolism threshold for catastrophic hydraulic failure in angiosperm trees. *Tree Physiology* 33: 672–683.

Warton DI, Duursma RA, Falster DS, Taskinen S. 2012. SMATR 3 – an R package for estimation and inference about allometric lines. *Methods in Ecology and Evolution* 3: 257–259.

Woo NS, Badger MR, Pogson BJ. 2008. A rapid, non-invasive procedure for quantitative assessment of drought survival using chlorophyll fluorescence. *Plant Methods* 4: 27.

Yao J, Sun D, Cen H, Xu H, Weng H, Yuan F, He Y. 2018. Phenotyping of *Arabidopsis* drought stress response using kinetic chlorophyll fluorescence and multicolor fluorescence imaging. *Frontiers in Plant Science* 9: e603.

Zhang Q, Bartels D. 2018. Molecular responses to dehydration and desiccation in desiccation-tolerant angiosperm plants. *Journal of Experimental Botany* 69: 3211–3222.

Zia A, Walker BJ, Oung HMO, Charuvi D, Jahns P, Cousins AB, Farrant JM, Reich Z, Kirchhoff H. 2016. Protection of the photosynthetic apparatus against dehydration stress in the resurrection plant *Craterostigma pumilum*. *The Plant Journal* 87: 664–680.

Supporting Information

Additional Supporting Information may be found online in the Supporting Information section at the end of the article.

Fig. S1 Total chlorophyll concentration during leaf dehydration based on SPAD measurements.

Fig. S2 Leaf functional impairment over a gradient of decreasing total relative water content (RWC) for the ten measured species

Table S1 Pressure-volume curve parameters for 10 analyzed angiosperm species.

Table S2 Dataset containing all variables measured for 10 analyzed angiosperm species.

Table S3 Model results for the determination of leaf relative water content (RWC) inducing percentage loss of rehydration capacity (*PLRC*).

Table S4 Model results for the determination of total relative water content (RWC) inducing percentage loss of maximum quantum yield of PSII (*PLCF*) under different irradiance.

Table S5 Results of the linear mixed-effect model analysis for chlorophyll fluorescence responses during leaf dehydration and rehydration.

Table S6 Independent *t*-tests for differences in RWC thresholds of leaf drought tolerance traits.

Table S7 Independent *t*-tests for differences in Ψ_{leaf} thresholds of leaf drought tolerance traits.

Table S8 Correlations between RWC indices of leaf functional impairment.

Table S9. Correlations between Ψ_{leaf} indices of leaf functional impairment.

Table S10 RWC thresholds of drought tolerance traits.

Table S11 Ψ_{leaf} thresholds of drought tolerance traits.

Please note: Wiley Blackwell are not responsible for the content or functionality of any Supporting Information supplied by the authors. Any queries (other than missing material) should be directed to the *New Phytologist* Central Office.